SYNTHESIS AND PERFORMANCE EVALUATION OF COVALENT ORGANIC FRAMEWORK NANOFILTRATION MEMBRANE FOR PER-AND POLYFLUOROALKYL SUBSTANCES REMOVAL

by

Ho-Kuan Yu.

A Thesis Submitted in

Partial Fulfillment of the

Requirements for the Degree of

Master of Science

in Engineering

at

The University of Wisconsin-Milwaukee

August 2022

ABSTRACT

SYNTHESIS AND PERFORMANCE EVALUATION OF COVALENT ORGANIC FRAMEWORK NANOFILTRATION MEMBRANE FOR PER-AND POLYFLUOROALKYL SUBSTANCES REMOVAL

by

Ho-Kuan Yu

The University of Wisconsin-Milwaukee, 2022
Under the Supervision of Professor Xiaoli Ma

Per- and polyfluoroalkyl substances (PFAS) have attracted the attention of many scientists due to their harm to the human body and the challenge in removing them from water. This thesis discusses the synthesis of covalent organic framework (COF) nanofiltration membranes and their PFAS removal performance. COF membranes were prepared by interfacial polymerization on polymer supports. The effects of synthetic parameters including concentration of monomers in the water phase and organic phase, soaking time, and reaction time on membrane structure and separation property were studied in this research. FTIR, SEM, and confocal microscopy were used for membrane characterization. It was found that increasing 2,4,6-trihydroxybenzene-1,3,5-tricarbaldehyde (Tp) monomer concentration and reaction time reduced the number of defects on the membrane surface and increased the membrane thickness. The change in the membrane surface morphology and thickness is less evident when varying the 2,5-dimethyl-1,4-phenylenediamine (Pa-2) concentration and soaking time. Membrane synthesized using a long reaction time of 120 seconds exhibited the lowest pure water flux and highest PFOS rejection.

Keywords: Interfacial Polymerization, Covalent Organic frameworks (COF), Nanofiltration Membrane, Per-and Poly- Fluoroalkyl Substances (PFAS)

To

my parents,

my family,

and my love

TABLE OF CONTENTS

LIST OF FIGURES

Chapter 1

Chapter 2

Chapter 3

LIST OF TABLES

Table 2

Table 3

ACKNOWLEDGMENTS

First, I would like to thank my advisor, Dr. Xiaoli Ma, for giving me a lot of help with research and everything else in life. When I decided to study abroad, I appreciated Dr. Ma's assistance, especially when having a hard time applying for a student visa in Taiwan. However, several hours of time lag exist between the U.S. and Taiwan. Dr. Ma always helps me overcome the upcoming task to arrive in the U.S. smoothly. When doing experiments, he gave us lots of new ideas and patiently discussed the result. He shows his professionalism in material science but still keeps us thinking independently.

Second, I would like to thank all of my family members and my girlfriend. Especially to my mom, dad, and sister for supporting me in studying aboard. Also, Thank you to my girlfriend Chiang-An, for all her love and support. Without their help, I would never finish all of this thoroughly.

Next, thanks to all of the others that have helped me before. Thank you for Dr. Lee and Dr. Tasi's understanding; Dr. Church and Dr. Wang are willing to be on my master defense committee without hesitation; Zhiqin, Weiling, Miguel, Rahul, and Xiaopeng for supporting any help with the experiment; all of the friends met in UWM that brings me lots of joy and let me feels like at home; those who helped me before.

Thank you!

CHAPTER 1

INTRODUCTION

1.1 Background

With the rapid growth of technology and the economy after the 20th century, the progress of society has also brought many challenges. In industries such as petrochemical, food, aerospace, automotive, construction, electronics, etc., wastewater is a part that we cannot ignore [1-3]. The wastewater comes from different industrial fields and contains various pollutants, heavy metals, organic, and chemicals. The annual population growth and climate extremes lead to water shortages and scarcity, the earth's water resources will soon be unable to meet the needs of modern human beings for water. Recycling and reusing wastewater plays a vital role in overcoming the lack of water sources. Through the efforts of scientists, many methods for treating wastewater have been found, such as biological trickling filters, chemical oxidation, activated sludge, and microalgae treatment[4-6].

Among different separation methods, membrane technology has become one of the focus research projects of scientists in these decades. Membrane-based separation has high efficiency and less energy consumption than traditional separation procedures. Membranes are also well suited for the separation or purification of materials that are sensitive to temperatures. In addition, membrane can overcome the azeotrope of two substances and separate[7]. The design of membrane and module can have different application areas according to different needs. The operating principle is simple and easy to be combined with other separation systems. Its small equipment space, easy operation, simple structure, and easy maintenance endow membrane separation technology with considerable potential and prospects in the industry[8].

1.2 Membrane Technology

Membranes have been used in various industries, including semiconductors, electronics manufacturers, coating technology, textile dyeing and finishing factories, biomedical pharmaceutical factories, etc.[9, 10]. A membrane is a semi-permeable membrane with selectivity that acts as a barrier layer between two phases and provides selectivity based on the membrane's physical or chemical properties, allowing a specific substance component to be separated from the remaining.

Polymers are easy to process and low-cost, and so are the common materials in membrane technology. Membranes can be sorted into different categories. According to the pores on the membrane, they can be divided into dense membranes and porous membranes; according to the membrane cross-section structure, they can be divided into the symmetric and asymmetric membranes; according to the morphology of the membrane itself, it can be divided into flat sheet and hollow fiber membranes; according to the affinity of the membrane surface for water, it can be divided into the hydrophilic and hydrophobic membranes; according to the ionic type of the membrane surface, it can be divided into the negatively charged and positively charged membranes.

1.3 Nanofiltration Membrane

Membrane filtration technology is driven by pressure difference for separation, and it is widely used in industry for solution concentration, solvent purification, separation or recovery of heavy metals, etc. According to the size of the pores on the membrane, applications can be divided into four categories, microfiltration, ultrafiltration, nanofiltration, and reverse osmosis. The separation mechanisms required by different applications are also different[11].

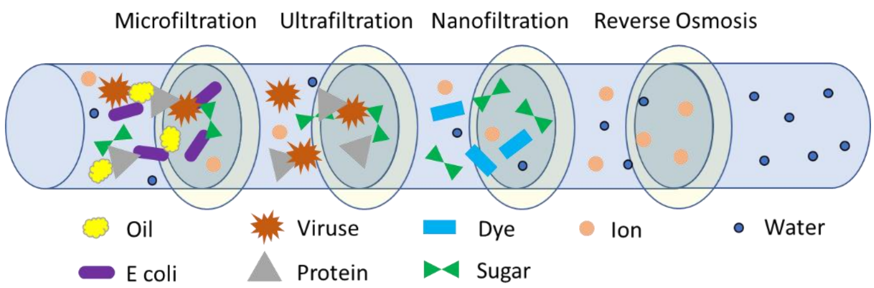

Figure 2. 1 Schematic diagram of membrane filtration application.

It is worth mentioning that nanofiltration is the last defined separation procedure among the four pressure-driven membrane separation procedures. Nanofiltration membrane is a process between ultrafiltration membrane and reverses osmosis membrane. Its molecular weight cut-off is between 200-1000 Dalton, and the membrane pore size is between 0.5-2 nm[12, 13]. Nanofiltration membranes are charged membranes, unlike ultrafiltration membranes and reverse osmosis membranes. Most nanofiltration membranes are negatively charged in a neutral or alkaline operating environment and positively charged in acidic. Its separation mechanism is usually dominated by the sieving or Donnan effect competing with each other.

1.3.1 Sieving effect

The sieving effect refers to the separation of the feed mixture through the size of the pores in the membrane. Since dissimilar substances have different volumes, hydration radii, kinetic diameters or other physical properties. The pore selection of the membrane needs to be between the sizes of the substances to be separated. After the mixture passes through the membrane, the material with a larger size will be blocked in front of the membrane, while the material with a smaller size can pass through the membrane smoothly to complete the separation of substances[14, 15].

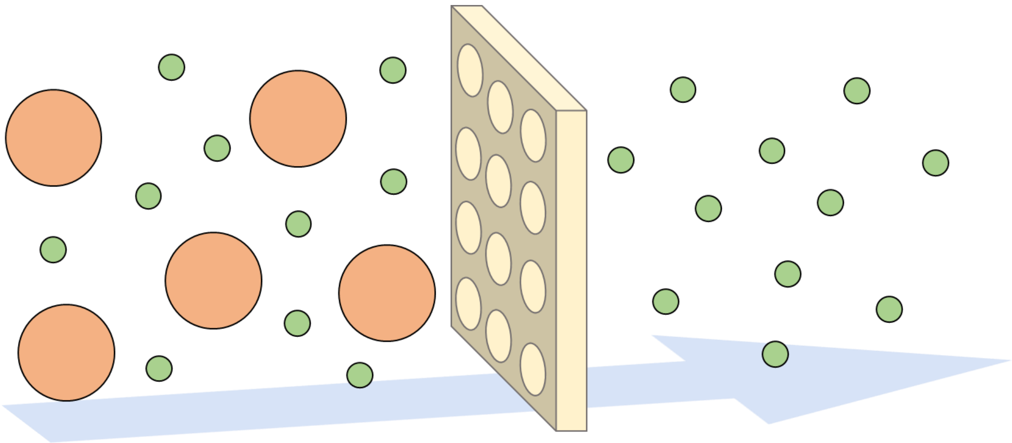

Figure 2. 2 Schematic diagram of sieving effect.

1.3.2 Donnan effect

There are many different chemical functional groups on the membrane, and these functional groups are charged due to the behavior of protonation or dissociation, so that the membrane has a positive or negative charge. The surface charge of the membrane will have a repulsive effect on ions with the same charge in water, and the repulsive force increases with the increase of the ion valence. The ions cannot pass through the membrane due to the effect of the repulsive force. In order to maintain the electrical neutrality of the mixture, the repelled ions will attract ions with different charges, so that the ions with different charges from the film cannot pass through the membrane[16, 17].

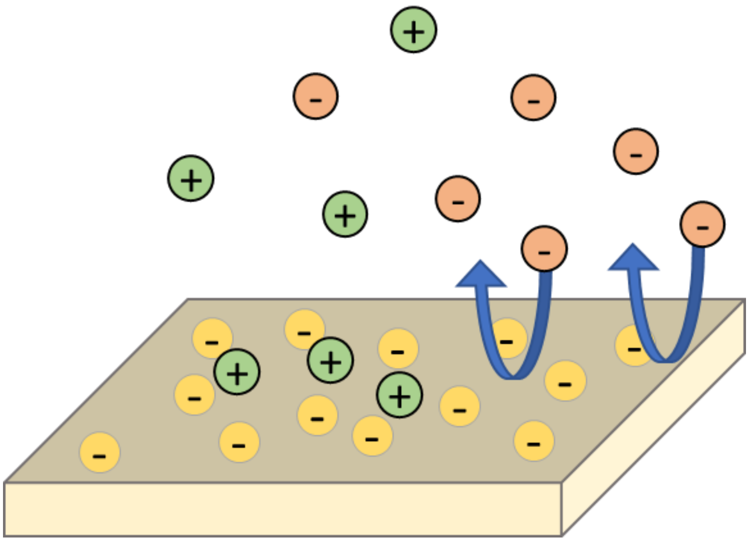

Figure 2. 3 Schematic diagram of Donnan effect.

1.3 Covalent Organic Framework

Covalent organic frameworks (COFs) are newly discovered crystalline and porous network materials which Yaghi and co-workers first found in 2005[18]. They are made up of organic linkers that form covalent bonds. Their massive and unique structures have attracted scientific interest recently. The atomically accurate spatial assembly of molecular organic building blocks provided huge potential design space for COF material[19]. COFs are an excellent suit for efficient separation processes due to their tunable pore structure and defined pore size[20]. It can be tuned explicitly by introducing various functional sites on the organic linkers and controlling interactions in an attractive or repulsive way[21].

COFs can be separated into two-dimensional (2D) and three-dimensional (3D) structures, two categories based on the varied dimensions of the covalently bonded frameworks. In 2D COFs, the covalent bonds were only formed in conjugated 2D sheets, and π-π stacking, hydrogen bonds, or van der Waals' force were formed between different 2D sheets. On the other hand, 3D COFs were connected to the entire 3D skeleton with covalent bonds[22].

β-ketoenamine-linked 2D COFs have high stability and are promising materials for membrane applications. Two β-ketoenamine-linked COFs, named TpPa-1 and TpPa-2, can be prepared by the reaction betwen 1,3,5-triformylphloroglucinol (Tp) and benzene- 1,4- diamine (Pa-1) and 2,5-dimethylbenzene-1,4- diamine (Pa-2), respectively (Figure 1. 1). The difference between them is that Pa-2 monomer has one more methyl group than the Pa-1 monomer. The methyl group will be appended in the pore channel of TpPa-2 COF affecting the pore size and pore chemistry property. The theoretical pore size of TpPa-1 and TpPa-2 are 1.8 and 1.5nm, respectively. In this research, we used TpPa-2 as the membrane material because its smaller pore size may lead to improved membrane rejection capability.

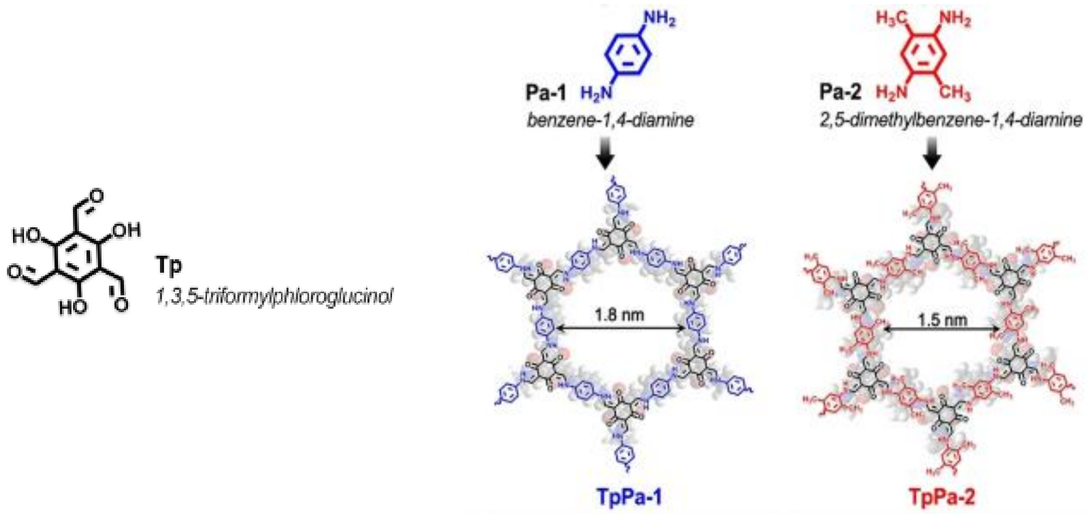

Figure 1. 1 Schematic of COF and monomers[23].

1.4 Polyfluoroalkyl and Perfluoroalkyl Substances (PFAS)

Poly and perfluoroalkyl substances are a significant category of anthropogenic aliphatic compounds. Since 1950, PFASs, surfactants and those polymers made with the aid of PFASs have been widely used in several manufacturing and commercial applications. A perfluoroalkyl moiety's chemical and thermal stability and hydrophobic and lipophobic properties result in very beneficial and long-lasting features in surfactants and polymers [24]. PFAS have been utilized in various formulations as surfactant intermediates, military bases, and waterproofing treatments for textiles and household products[25, 26]. As a result, PFASs have been discovered in different kinds of urban water cycles, including wastewater, river water, lake water, and even drinking water [27-31]. Even though current legislation restricts their usage, perfluorooctanoic acid (PFOA) and perfluorooctane sulfonic acid (PFOS) are the most commonly detected in the aquatic environment. The human body will absorb PFASs by oral ingestion, which cannot be metabolized. They've been found in human tissue and blood and will be stored preferentially in the liver[26]. According to studies, thyroid disease, excessive cholesterol, ulcerative colitis, kidney cancer, testicular cancer, and pregnancy-induced hypertension are all connected to the presence of PFOA and PFOS in people[32-34].

Removing PFASs in the water is a challenging task due to the high strength of the C–F covalent bond in their chain, usually low concentration in water [35, 36]. In addition, it can separate into two categories depending on where to operate the harmful chemicals, ex-situ and in-situ PFAS groundwater treatment technologies[37, 38].

1.4.1 Ex-Situ PFAS Groundwater Treatment Technology

(1) Adsorption

Adsorption process is an efficient approach for removing PFOS and PFOA from wastewater. Effective adsorbents have been identified, such as activated carbon, resin, chitosan, hydrotalcite, alumina, and organo-montmorillonite[39, 40].

(2) Molecularly Imprinted Polymer (MIP)

Molecular imprinting is a technique for creating polymeric materials that act as specific molecular recognition receptors. MIPs are formed by polymerizing template species and monomers in the presence of cross-linkers and polymerizable complexes, resulting in binding sites that complement the template molecule[41].

(3) Filtration

Microfiltration, ultrafiltration, nanofiltration, and reverse osmosis membranes are some of the several types of membranes that may be used to treat PFAS. Nanofiltration and Reverse osmosis membranes are potentially more appropriate for PFAS filtering due to the ideal pore diameters of 1–10 nm and less than 1 nm, respectively[37].

(4) Sonochemical Destruction

Sonochemistry refers to using an acoustic field to generate chemical reactions in a solution. Cavitation occurs when sound waves collide with the bubbles in a solution, causing high vapor temperatures and pyrolytic breakdown of PFASs at the bubble-water interface. Ultrasound frequencies used in the sonochemical treatment of PFASs typically vary from 20 to 1000 kHz or more than 0.5 MHz[42].

1.4.2 In-Situ PFAS Groundwater Treatment Technology

(1) Bioremediation

The employment of a biological agent to break down toxins, known as bioremediation, could be a straightforward, environmentally safe, and cost-effective way to treat PFAS-contaminated soils. Bioremediation has been effectively used to remove a number of organic contaminants from the environment, including petroleum hydrocarbons, chlorinated chemicals, and pesticides.[43]

(2) Chemical Oxidation

Advanced oxidation processes (AOPs) are the focus of developing in situ chemical oxidation (ISCO) technologies for PFASs. Hydrogen peroxide, sodium persulfate, potassium/sodium permanganate, ozone, and ozone/peroxide are all common ISCO reagents.

(3) Chemical Reduction

While reductive dehalogenation appears to be a viable route for PFAS destruction. To treat contaminants, reduction methods use either direct electron transfer or the formation of reactive free radicals, which then degrade the pollutants. Zero-valent metals and sodium dithionite are two common reductants that have been tested so far[44].

(4) Treatment Train Approaches

Treatment trains that combine complementary technologies to allow for in-situ cleanup may be more successful than single technologies. To improve the performance of eliminating hazardous substances, combine two or more of the therapies indicated above.

1.5 Literature Review

Per- and poly-fluoroalkyl substances (PFASs) are a category of at least thousands of harmful artificial chemicals. They have been widely used in different industrial sectors and tons of daily consumer products, including food packaging, household products, waterproof fabrics, and non-stick cookware since the 1950s[45].

Kucharzyk et al. sorted out the ways of how scientists deal with the PFAS problem. The method was separated into two categories depending on where the process was taken, in and ex-situ groundwater treatment. There are many ways, including sorption, filtration, sonochemical destruction, chemical oxidation, and reduction [37]. Mohamed et al. combined the advantages and disadvantages of PFASs removal methods. Most research focused on long-chain PFAS such as PFOA and PFOS. However, short chains of PFASs are also exists in the environment wastewater, and more studies should be reported.

Lee. et al. reported summaries on the membrane technologies for PFAS removal. In this article, nanofiltration and reverse osmosis membrane were mentioned and reviewed. Many researches show high performance for PFAS rejection. Developing a membrane with higher recovery to overcome the generation of membrane concentrate is a big challenge for now. Designing a treatment train to deal with the weakness of various individual methods can let the system stay longer and become more efficient[46].

Chuyang et al. reported several nanofiltrations and reverse osmosis membranes used to remove the PFAS compound. The reverse osmosis membrane showed higher rejection >99%, nanofiltration membrane has a lower rejection but is still good from 90 to 99%. They found out the rejection would be higher after a period of operation because of PFOS entrapped in the polyamide selective layer[47].

Wang. et al. using dry-wet inversion technique to fabricate a PMIA negative charged hollow fiber nanofiltration membrane. In higher pH value showed a higher PFOS rejection of 97.49% than the lower pH value of 91.17%. Moreover, a higher Ca^{2+} concentration increases the rejection of PFOS due to improving the molecular polarity and also increases the molecule size of PFOS. [48].

Wang et al. reported the membrane rejection mechanism for the PFAS system in the research, including the solute concentration, molecular size, ionic strength, and membrane pore size. In addition, they mentioned in the earlier step that the dominant rejection mechanism for PFOS was adsorption. After the fouling cake become thicker, the rejection mechanism was governed by size exclusion[49].

Tin et al. incorporated MXene nanosheets into the aqueous phase during interfacial polymerization of the polyamide layer when loading 0.025 wt% of MXene. The TFN hollow fiber nanofiltration membrane increased its PFOS by about 20%, while the flux of the hollow fiber membrane also improved[50].

1.6 Research Objective

After decades of using PFAS, they have been found in many different urban water cycles, including wastewater, river water, lake water, and even drinking water. Scientists have reported this serious problem of our human body absorbing PFAS, including thyroid disease, excessive cholesterol, ulcerative colitis, kidney cancer, testicular cancer, and pregnancy-induced hypertension. Finding a suitable and effective method to overcome the problem is an urgent goal now.

This research aims to develop high-flux covalent organic framework (COF) nanofiltration membranes for PFAS removal. The objective is to investigate the effect of various synthetic parameters on the formation of COF membranes on commercial support and evaluate the membrane performances including water permeances and salt and PFAS rejections. The COF membrane will be obtained through the interfacial polymerization method. There were several parameters to control while synthesizing the COF membranes, including the concentration of the monomers, reaction time, concentration and type of catalyst, etc. Here we are using systematic research to find the most suitable parameter for fabricating TpPa-2 COF membrane.

CHAPTER 2

EXPERIMENT WORK

2.1 Materials

Polyether sulfone (PES) ultrafiltration membranes (50,000 Da) were purchased from Synder Filtration Inc. (United States) used as the support for COF membranes. The materials used in the COF synthesis are 2,5-dimethyl-1,4-phenylenediamine (Pa-2, 98%), acetic acid (99.7%), 2,4,6-trihydroxybenzene-1,3,5-tricarbaldehyde (Tp, 95%), hexane (95%). The salts used for testing nanofiltration performance were sodium sulfate (Na_2SO_4), magnesium sulfate ($MgSO_4$), magnesium chloride ($MgCl_2$), sodium chloride (NaCl). Pa-2 were obtained from Tokyo Chemical Industry CO., LTD.; Tp were purchased from Ambeed Inc.; and the others were supplied by Sigma Aldrich Inc.

Table 2. 1 PFASs used in this research.

Per and polyfluoroalkyl substances (PFAS)	Molecular weight (g/mol)	Chemical structure
Perfluorobutanesulfonic acid (PFBS)	300.10	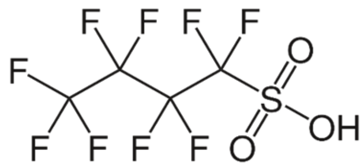
Perfluorooctanoic acid (PFOA)	414.07	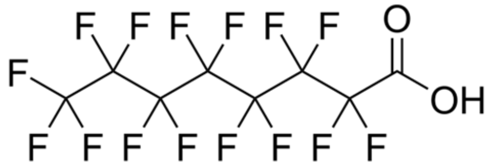
Perfluorooctanesulfonic acid (PFOS)	500.13	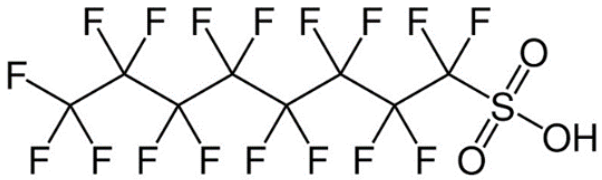

2.2 COF Membrane Fabrication

2.2.1 Preparation of Aqueous and Organic Phase Solution

The aqueous solutions were prepared by dissolving various amounts of Pa-2 monomer in DI water with an acetic acid catalyst. The catalyst was added to the solution with a constant ratio of 1:100 to DI water. Aqueous solutions were mixed by vortex mixer and frequently checked by visual observation under room light sources to ensure the monomer dissolved entirely. Afterward, various amount of Tp monomer was dispersed in hexane solution by ultrasonic treatment for 10 minutes and checked by lifting under room light sources to ensure it dissolved completely.

2.2.2 COF Membrane Synthesis

The PES support was soaked in DI water overnight before synthesis. The support was clipped on a 2.5-inch square glass plate and removed residual water on the surface with the hand squeeze bulb. A polytetrafluoroethylene (PTFE) mold was fixed on the support to control the reaction area. 5 ml aqueous solution was added to the mold using a pipette. The mold was covered with another glass plate to avoid the solution from evaporating. After a required time of keeping the aqueous solution on the support, the mold and the solution were removed from the support simultaneously. The residual solution on the membrane was removed again in the same way. At last, 5ml of the organic solution was added to the surface of the support. After the required reaction time, the membrane was washed with 3ml hexane for three rounds. The membrane was then washed with DI water and stored in water for later use.

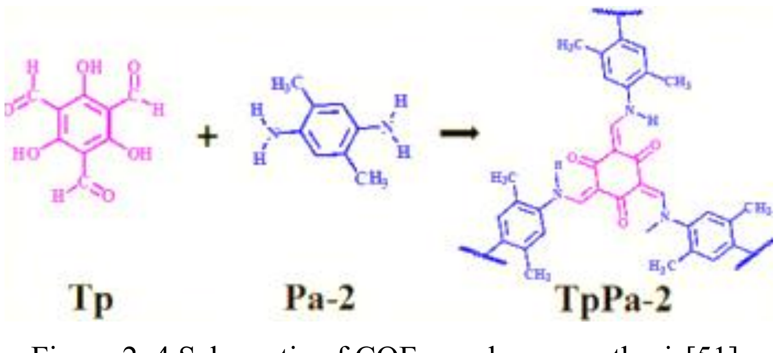

Figure 2. 4 Schematic of COF membrane synthesis[51].

2.3 Membrane Characterization

2.3.1 Membrane Thickness Measurement

The membrane was cut into small pieces and clipped between two glass slides. Two glass slides were bond with a PTFE (Polytetrafluoroethylene) tape. Then the module was soaked in DCM (Dichloromethane) in the fume hood for 2 hours. The DCM will dissolve the support, which is polyether sulfone used in this research. After the polymer support was completely dissolved, DCM was filled into the gap between two glass slides to remove the residual polymer solution. Insert a blade into the aperture between two glass to open it. Drop more DCM can make it easier. Let it dry after complete making the samples and the thickness were measured by confocal microscope.

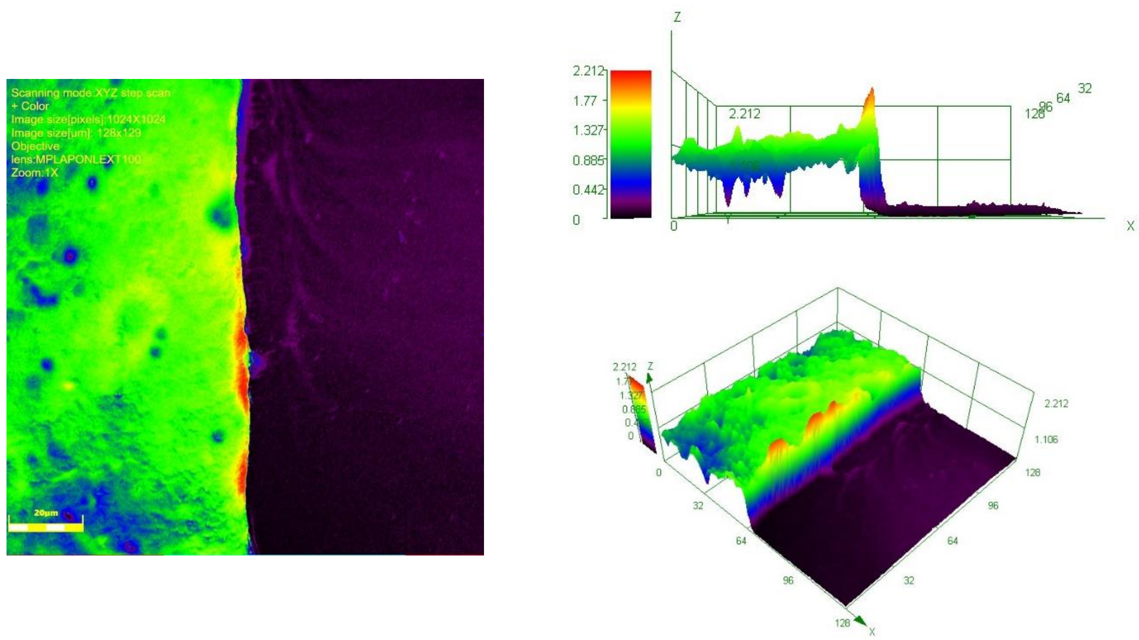

Figure 2. 5 Schematic of thickness measurement by using the confocal microscope.

2.3.2 Pure Water Flux and Nanofiltration Filtration Test

The pure water flux and nanofiltration performance of the prepared membranes were tested by a homemade crossflow nanofiltration setup. The following solutions were used in the feed tank (a): (1) distilled water, (2) 2000ppm saltwater solution, (3) PFAS water solution. The feed flow rate was maintained at 0.8 LPM (Liter per minute, L/min). The membranes were compacted using DI water under a feed pressure of 80 psi to stabilize the membrane performance. After the compaction, the water permeate was collected for 5 minutes under 60 psi to calculate the membrane flux. The conductivity meter measured the salt concentration in the feed and permeate to calculate the salt rejection. HPLC was used for testing the PFAS concentrations of feed and permeate solutions to calculate the rejection. The water permeance and solute rejection (for salt and PFAS) were calculated with the following formula:

$$\text{Water permeance (F)} \quad \mathrm{F(LMH/bar)} = \frac{V}{A \times t \times P}$$

$$\text{Rejection (R\%)} \quad \mathrm{R\%} = \left(1 - \frac{C_p}{C_f}\right) \times 100$$

Were,

V： Permeance volume, (L)

A： Area exposed for separation (m2)

t： Sampling time (hr)

P: Operating pressure to the crossflow cell(bar)

Cp： Permeate concentration(ppm)

Cf： Feed concentration(ppm)

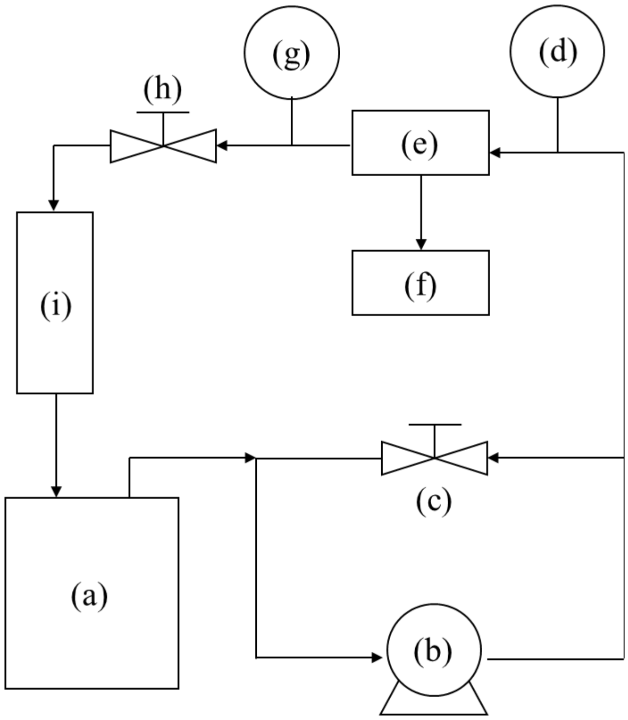

(a): Feed tank,

(b): Pump,

(c): Bypass valve,

(d): Inlet pressure gauge,

(e): Membrane testing module,

(f): Permeate collection,

(g), Outlet pressure gauge,

(h): Outlet valve,

(i): Flowmeter

Figure 2. 6 Schematic of pure water flux and nanofiltration cross flow experiment setup.

CHAPTER 3

RESULT AND DISCUSSION

3.1 Effect of Pa-2 Concentration on COF Morphology and Performance

Figure 3. 1 shows the microstructure of the PES support and the COF membrane fabricated on the support. Nanoscale pores with a high density can be observed on the support. However, as shown in the SEM surface image of the COF membrane, it was hard to find pores on the membrane surface because most of them were covered by the top COF membrane layer. This suggested that a continuous COF membrane layer was successfully formed from the interfacial polymerization reaction on the support surface.

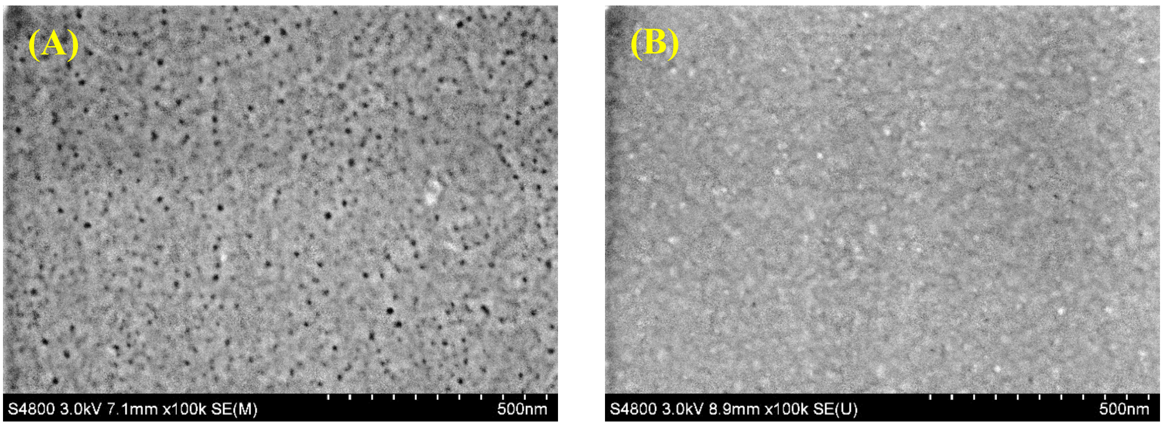

Figure 3. 1 SEM surface images of (A) support and (B) COF membrane.

Figure 3. 2 shows FTIR for Tp, Pa-2, COF, and support. The CH=O group from the Tp monomer showed at 2885cm^{-1}, Pa-2 monomer shows peaks from 3200 to 3400cm^{-1}. However, the peaks from Pa-2 and Tp monomers seemed to have disappeared on the COF membrane, suggesting the almost complete reaction between the monomers. In addition, compared to the support, two new peaks appeared in the COF membranes, one at 1574 cm^{-1} corresponding to the C=C stretching band and the other at 1250 cm^{-1} caused by C-N stretching[52]. These two peaks confirmed the successful synthesis of COF material on the support.

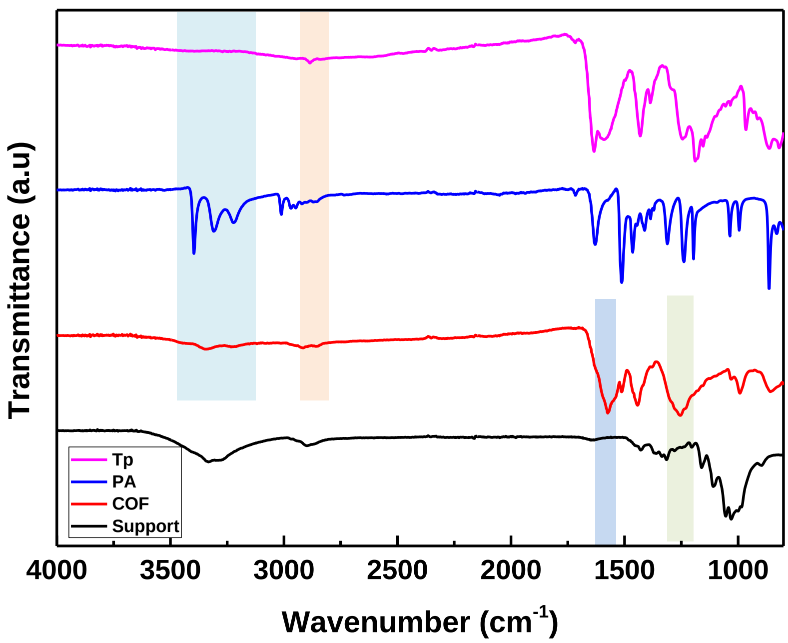

Figure 3. 2 FTIR spectrum for monomers and COF membrane.

As shown in Figure 3. 3, various Pa-2 concentrations (0.25, 0.5, 1, and 2wt%) were used to prepare COF membranes, while maintaining a constant Tp concentration (0.025 wt%), Pa-2 soaking time (30 s), and interfacial polymerization reaction time (30 s). In the digital photo, we noticed that the COF membrane has an obvious color change compared with the support. When the COF layer was fabricated on the support, it turned into light yellow or dark orange. Increasing the Pa-2 solution concentration has slightly made the color of COF membranes darker.

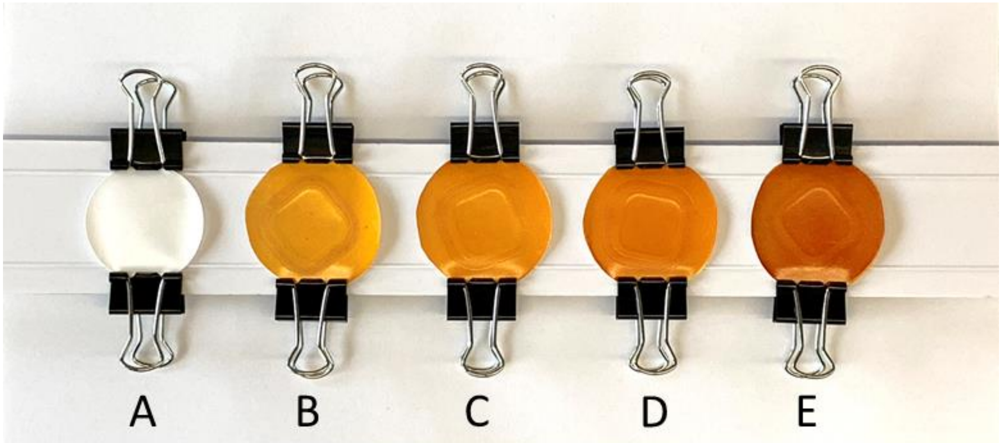

Figure 3. 3 Digital photo of various Pa-2 conditions COF membrane. (A) Support, (B) 0.25wt%, (C) 0.5wt%, (D) 1wt%, (E) 2wt%

SEM was used to characterize the surface morphologies of the membranes. In Figure 3. 4, pores can be observed in all four conditions of COF membranes. However, when the concentration of the aqueous Pa-2 solution increases, the number of pores on the surface of the membrane gradually decrease. This is because more Pa-2 monomers can adsorb on the support surface when the concentration increases. Then when the membrane is in contact with the organic-phase Tp solution, more COF materials can be formed on the support during the interfacial polymerization step. Therefore, higher Pa-2 concentration resulted in a higher degree of polymerization and a denser COF layer.

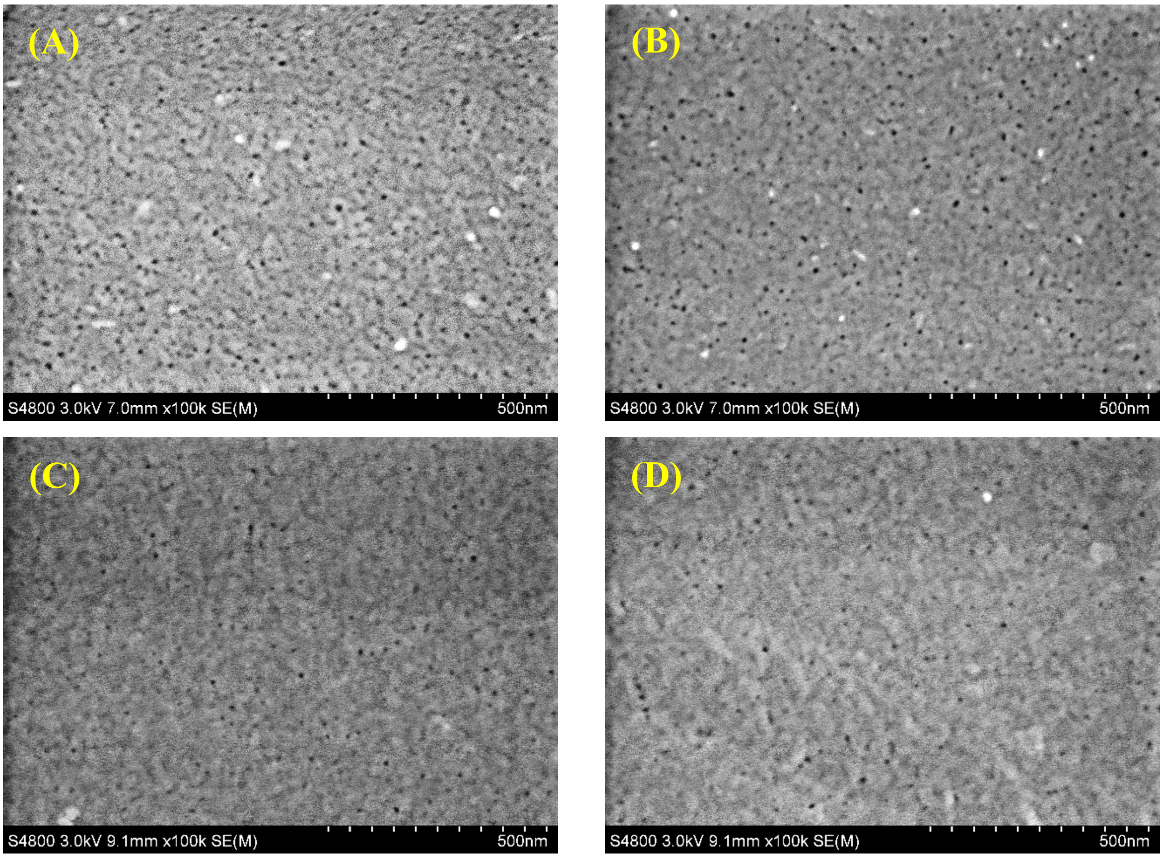

Figure 3. 4 Effect of Pa-2 concentration on SEM surface image. (A) 0.25wt%, (B) 0.5wt%, (C) 1wt%, (D) 2wt%.

Table 3. 1 shows the thickness of the COF layer on the support. The bulk composite membrane was immersed in dichloromethane to dissolve the PES support and then the COF membrane layer was transferred onto a glass slide. The thickness of the COF layer was measured by confocal microscopy. In the table, we noticed that Pa-2 concentration affected the thickness of the COF layer. The thickness slightly increased with increasing the concentration of Pa-2 solution. More Pa-2 monomers will exist in the solution at higher concentration conditions and react with Tp monomers of constant concentration, resulting in a gradual increase in the thickness of the membrane. The difference in thickness is consistent with the different colors observed for these membranes.

Table 3. 1 Effect of Pa-2 concentration on COF membrane thickness.

Pa-2 concentration (wt%)	Thickness (nm)
0.25	312±43
0.5	390±87
1	442±63
2	567±93

Figure 3. 5 shows the pure water flux of the COF composite membrane. It can be found that with the increase of Pa-2 concentration, the pure water flux of the membrane decreases accordingly. This is because it is observed in the SEM images in Figure 3. 4 that the size and the number of pores on the membrane surface tend to become smaller as the Pa-2 concentration increase. In addition, Table 3. 1 shows that the thickness of the membrane gets thicker with increasing Pa-2 concentration. Because of the reduction of the pore size and increase of membrane thickness, the resistance of water to pass through the membrane increases[49], leading to pure water flux gradually decreasing[53].

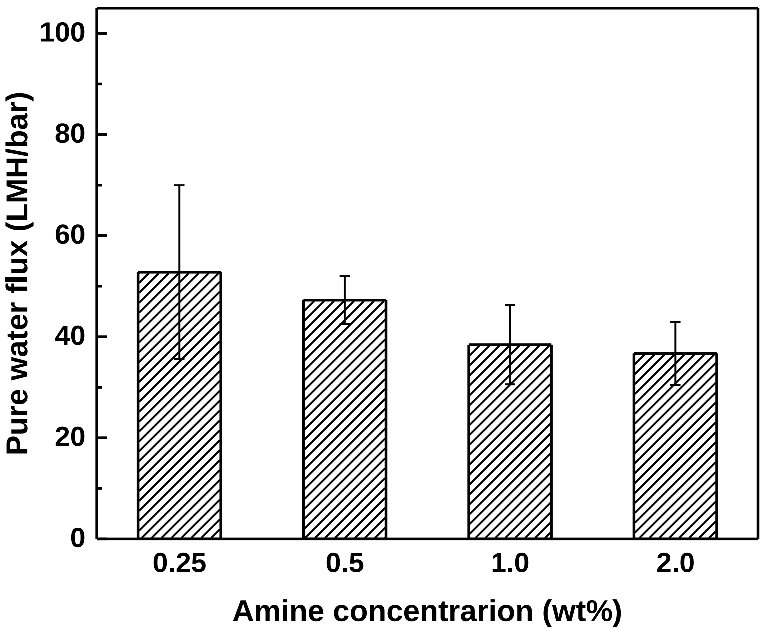

Figure 3. 5 Effect of Pa-2 concentration on pure water flux.

Figure 3. 6 shows the salt rejection performance of the COF membranes. It can be seen that the rejection of sodium sulfate increases with increasing the Pa-2 concentration. From the SEM and the thickness mentioned above turned into the resistance of the membrane becomes higher with increasing the Pa-2 concentration. The increase of the transfer resistance will also increase the rejection of the membrane to the solute. According to the sieving effect, the solutes are blocked upstream of the membrane.

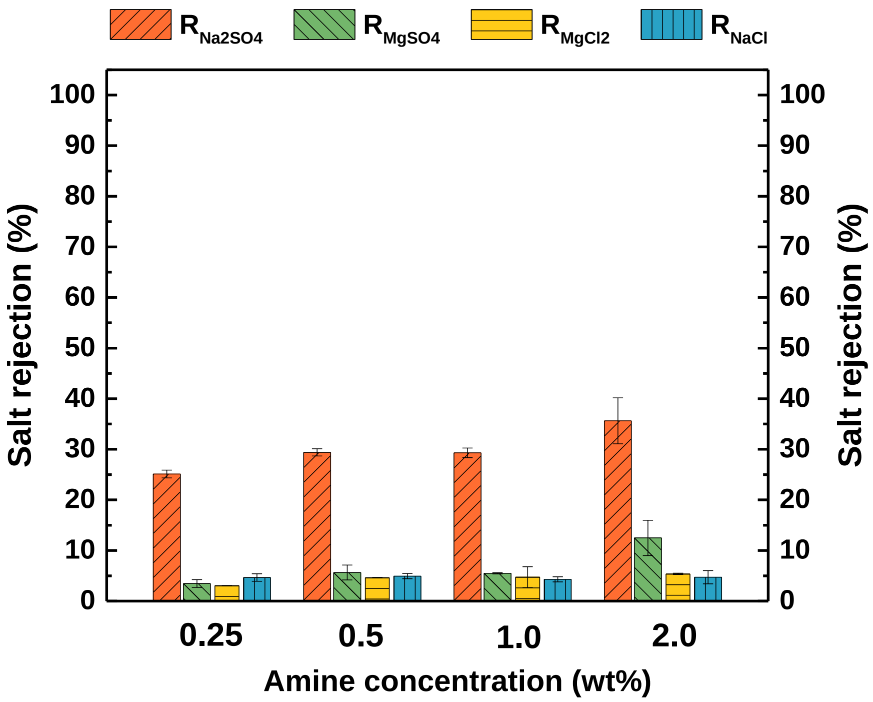

Figure 3. 6 Effect of Pa-2 concentration on salt rejection performance.

3.2 Effect of Pa-2 Soaking Time on COF Morphology and Performance

The Pa-2 soaking time was changed in this section. The conditions of Pa-2 soaking time were 30 seconds, 1, 2, and 4 minutes. The concentrations of Pa-2 solution were constant at 2wt%, Tp concentration was 0.025 wt%, and reaction time was kept at 30 seconds. In Figure 3. 7, we notice that the color of the COF membranes remains almost the same and shows a dark orange for all membranes.

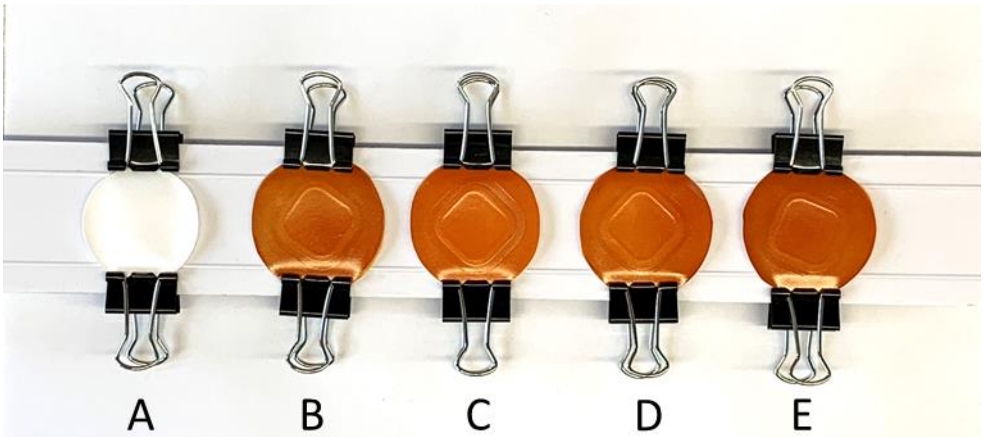

Figure 3. 7 Digital photo of various Pa-2 soaking times of COF membrane. (A) Support, (B) 0.5min, (C) 1min, (D) 2min, (E) 4min.

The SEM images of COF membranes made using various Pa-2 soaking times were shown in Figure 3. 8. Pores can be found in all conditions. However, the pore density and pore size decrease gradually as increasing the soaking time of supports with Pa-2 solution. With a longer time of letting the solution sit on the support, the solution penetrates the pores in the support. When the membrane was immersed in the Tp solution, not only on the surface but the inside the pores was formed by COF.

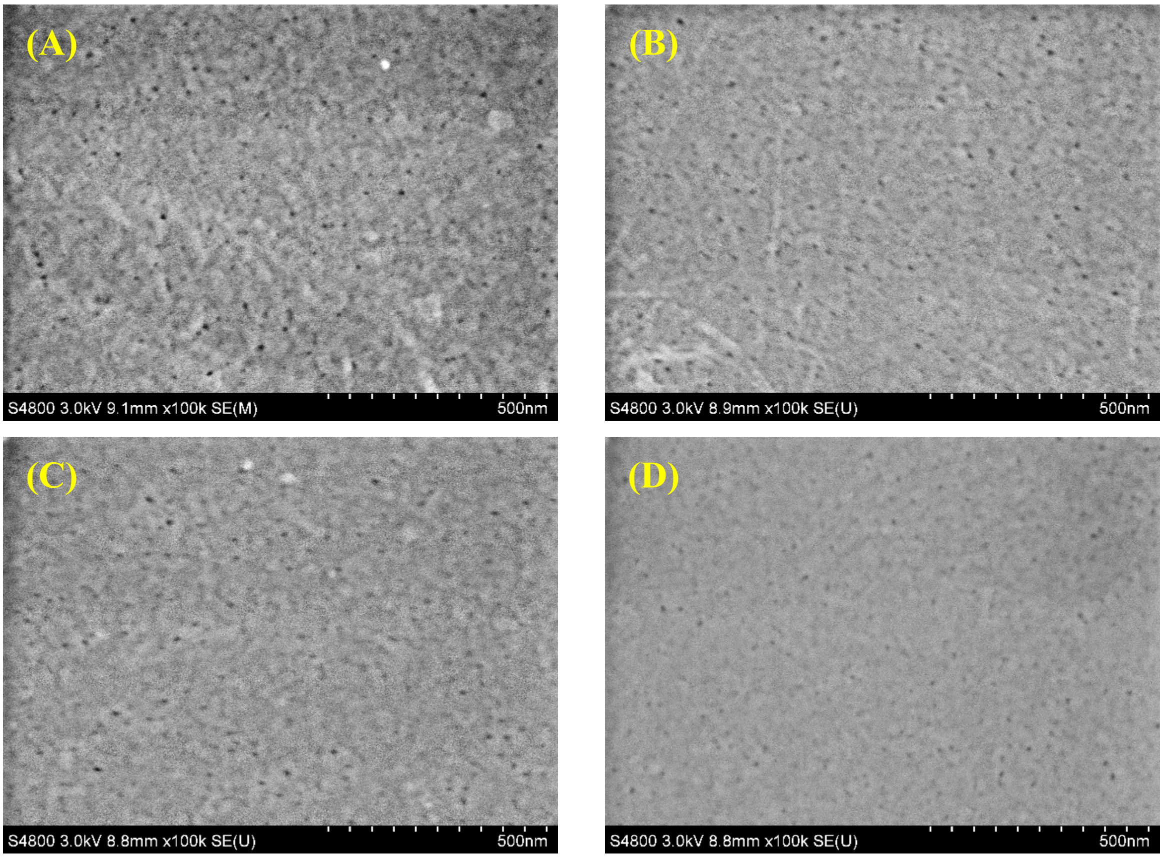

Figure 3. 8 Effect of Pa-2 soaking time on SEM surface image. (A) 0.5min, (B) 1min, (C) 2min, (D) 4min.

The thickness of membrane fabricated by different Pa-2 soaking times was listed in Table 3. 2. In the table, we can notice that the COF membrane's thickness almost remains the same. The membrane thickness keeps in the range of 550 to 600 nanometers, and there is no significant difference in each condition. Compared with the Pa-2 concentration, the change of Pa-2 soaking time does not affect the COF membrane thickness.

Table 3. 2 Effect of Pa-2 soaking time on COF membrane thickness.

Pa-2 soaking time (min)	Thickness (nm)
0.5	567±93
1	554±58
2	566±41
4	586±44

The pure water flux of various Pa-2 soaking times was shown in Figure 3. 9. In the figure, the change slightly increases and then decrease. However, if we include the experiment error bar of each condition in the discussion, the flux stays close to around 35 LMH/ bar. Therefore, the flux was not affected by the soaking Pa-2 time. This result can also be found in Table 3. 2. The membrane thickness does not change with increasing the Pa-2 soaking time. The thickness of the membrane determines the transport resistance of the membrane. In this case, the transport resistance remains the same, which then leads to the same flux for each condition.

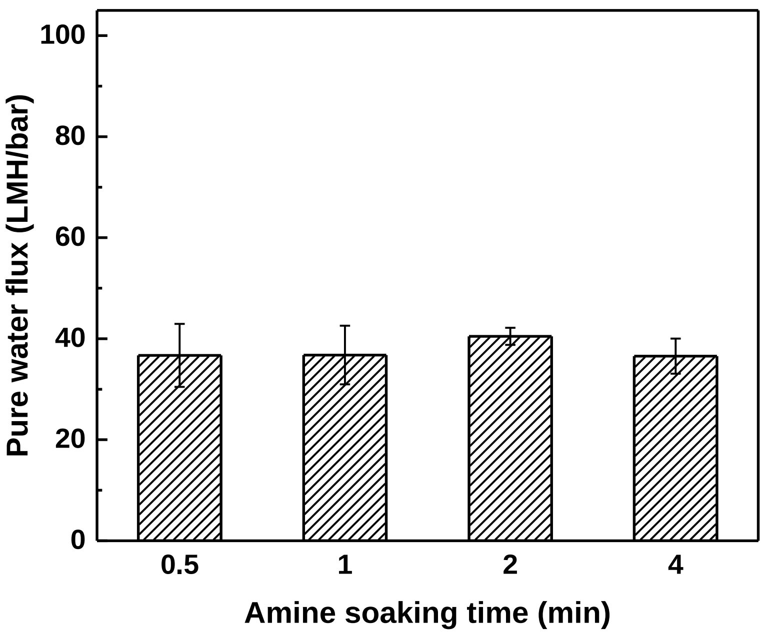

Figure 3. 9 Effect of Pa-2 soaking time on pure water flux.

The salt rejection of these COF membranes is shown in Figure 3. 10. Increasing the soaking time of Pa-2 does not affect salt rejection performance. The same result was shown in Table 3. 2 and Figure 3. 8. The thickness of the COF membrane remains the same, leading to the same solute resistance.

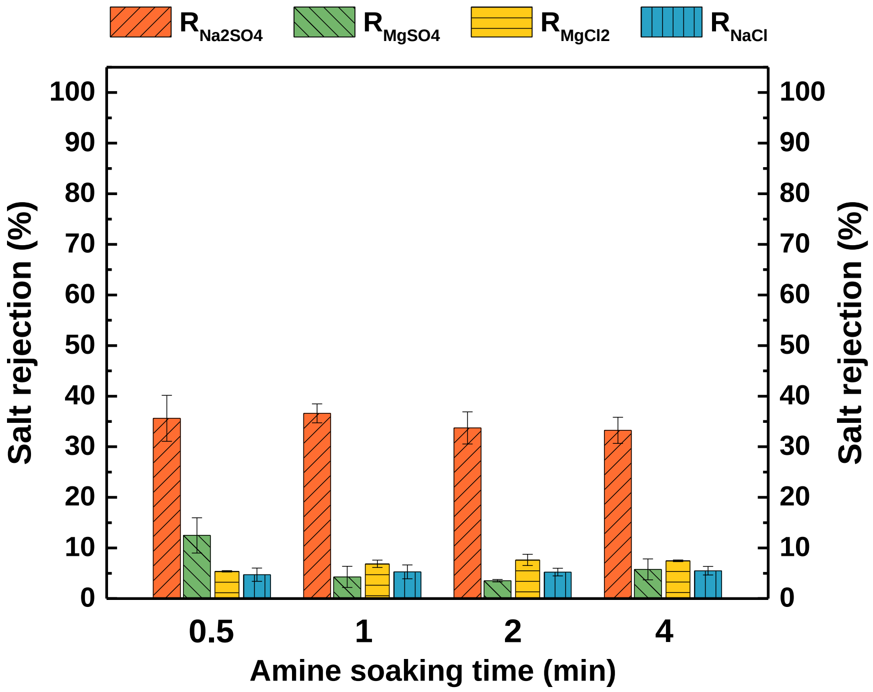

Figure 3. 10 Effect of Pa-2 soaking time on salt rejection performance.

3.3 Effect of Tp Concentration on COF Morphology and Performance

The Tp concentrations studied in this section were 0.0125, 0.025, 0.05, 0.1wt%. The other synthesis parameters were kept constant. The Pa-2 concentration was 2wt%, Pa-2 soaking time was 30 seconds, and the reaction time between Pa-2 and Tp was 30 seconds. Figure 3. 10 shows the digital photo of the COF membranes. The color gets darker when fabricating the COF membrane with a higher Tp concentration. The color changes from khaki yellow to orange when increasing the Tp concentration.

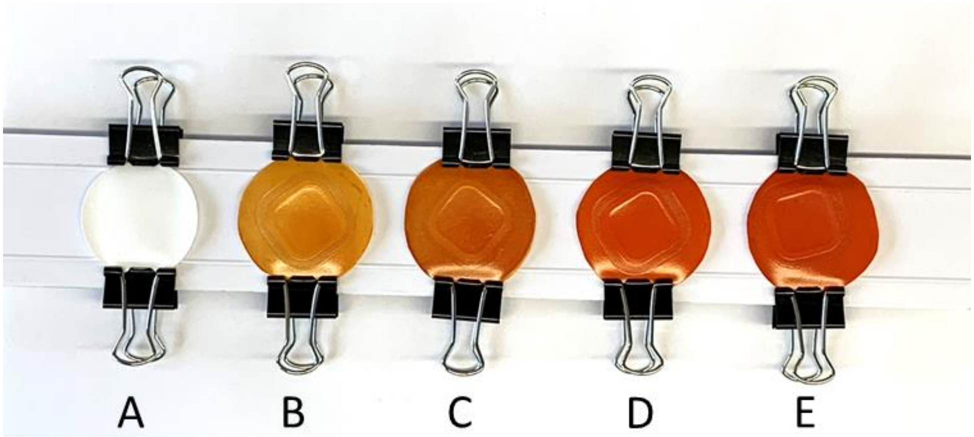

Figure 3. 11 Digital photo of various Tp concentration of COF membrane. (A) Support (B) 0.0125wt%, (C) 0.025wt%, (D) 0.05wt%, (E) 0.1wt%.

The COF membrane surface morphology is shown in Figure 3. 12. Here, large pores can be found in the first two conditions. However, pores become smaller when increasing the Tp concentration to 0.05wt%, decreasing pore density. As the Tp concentration was further increased to 0.1wt%, most pores disappear and are barely observed on the membrane surface. Pore size and pore density decrease because the higher concentration of Tp concentration provides more Tp monomers to react with Pa-2 monomer. In the chemical structure of Pa-2 and Tp monomers shown in Figure 2. 4, the Pa-2 monomer got two functional groups, and the Tp monomer got three. One monomer with more than three monomers can easily form a crosslinking structure with two functional group monomers. In this section, increasing the Tp concentration lets two monomers get more chance to react and leads to a higher crosslinking degree. With a higher crosslinking degree, more COF were formed on the membrane surface and covered the pores from the support.

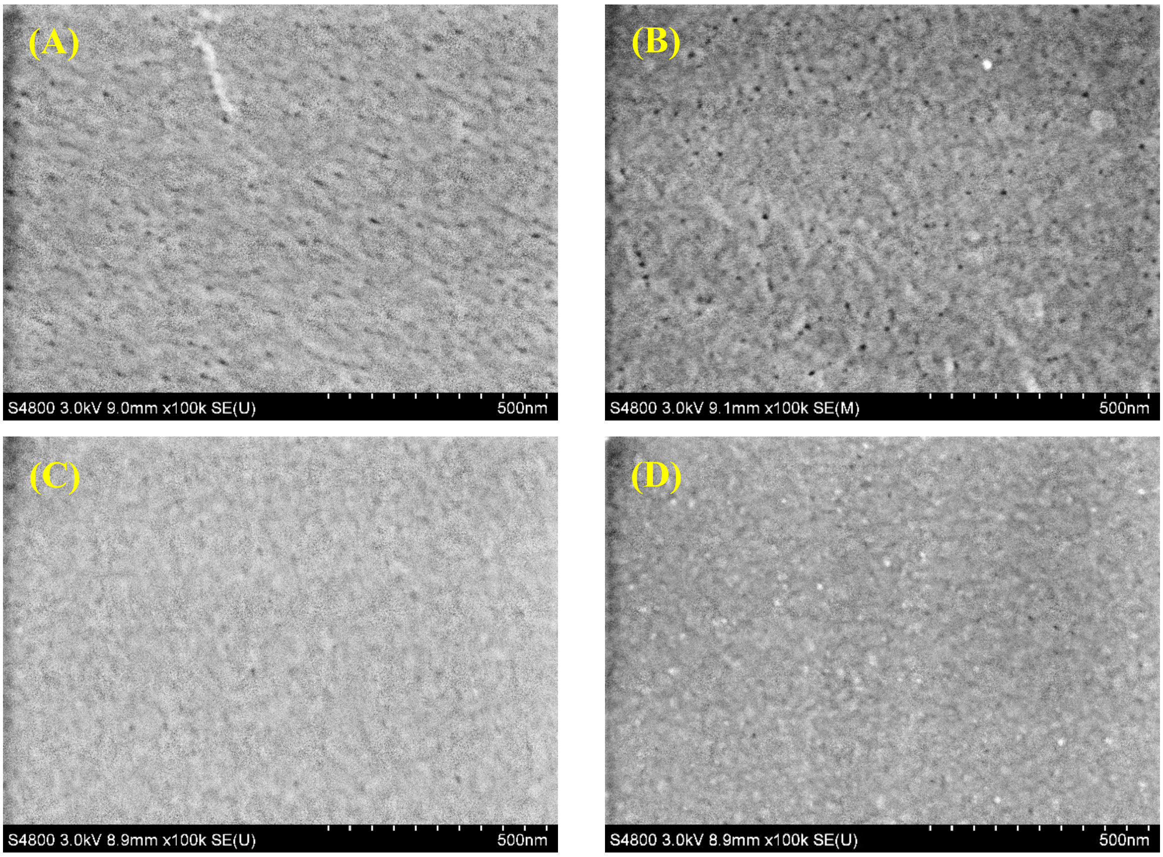

Figure 3. 12 Effect of Tp concentration on SEM surface image. (A) 0.0125wt%, (B) 0.025wt%, (C) 0.05wt%, (D) 0.1wt%.

The thickness of the COF membrane fabricated with different Tp concentration were listed in Table 3. 3. The thickness increases with increasing the Tp concentration. The membrane made using the highest Tp concentration is almost three time thicker than the one synthesized from the lowest Tp concentration. The thickness increase is because the higher Tp concentration can have more reaction between Tp and Pa-2 monomer. That will lead to a higher cross-linking degree for the COF membrane. Furthermore, the thickness result collected in Table 3. 3 can also prove the result in Figure 3. 12. More pores from the support can be covered with a thicker COF membrane layer synthesized using a higher Tp concentration.

Table 3. 3 Effect of Tp concentration on COF membrane thickness.

Tp concentration (wt%)	Thickness (nm)
0.0125	445±98
0.025	567±93
0.05	714±94
0.1	1392±71

Figure 3. 13 shows the pure water flux of COF membranes synthesized with different Tp concentrations. The flux decreases dramatically with increasing the Tp concentration. The membrane flux from the highest concentration was 2.5 times lower than the lowest concentration. As shown in Figure 3. 12 and Table 3. 3, tiny pores, low pore density, and thick membrane were all included in the COF membrane using 0.1wt% Tp concentration. All results suggest that this membrane has the highest transfer resistance. Therefore, under the same driving force of about 80 psi used in this research, this COF membrane has the lowest water permeance.

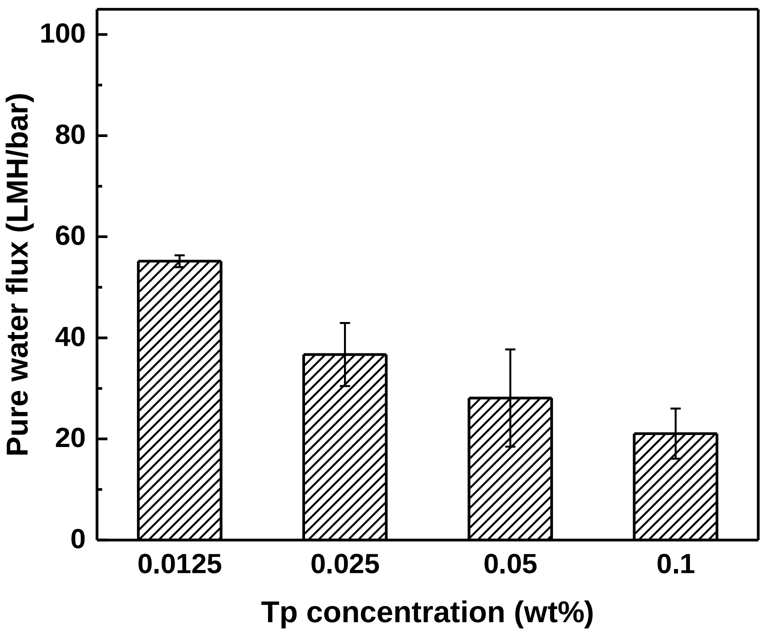

Figure 3. 13 Effect of Tp concentration on pure water flux.

Figure 3. 14 shows the salt rejection of the COF membrane. The rejection of sodium sulfate increases as the Tp concentration increases to 0.025 and then keeps constant. In addition, the rejection of magnesium sulfate keeps gradually growing from 2.95% to 17.38%. In Figure 3. 12, the pore sizes on the membrane surface decreased when increasing the Tp concentration. In Table 3. 3, the thickness of the COF membrane becomes thicker when using higher Tp concentration in the interfacial polymerization step. Due to these situations, the solutes in the feed solution were more challenging to pass through the membrane. In other hand, the salts were also hard to pass the membrane that lead to a higher rejection.

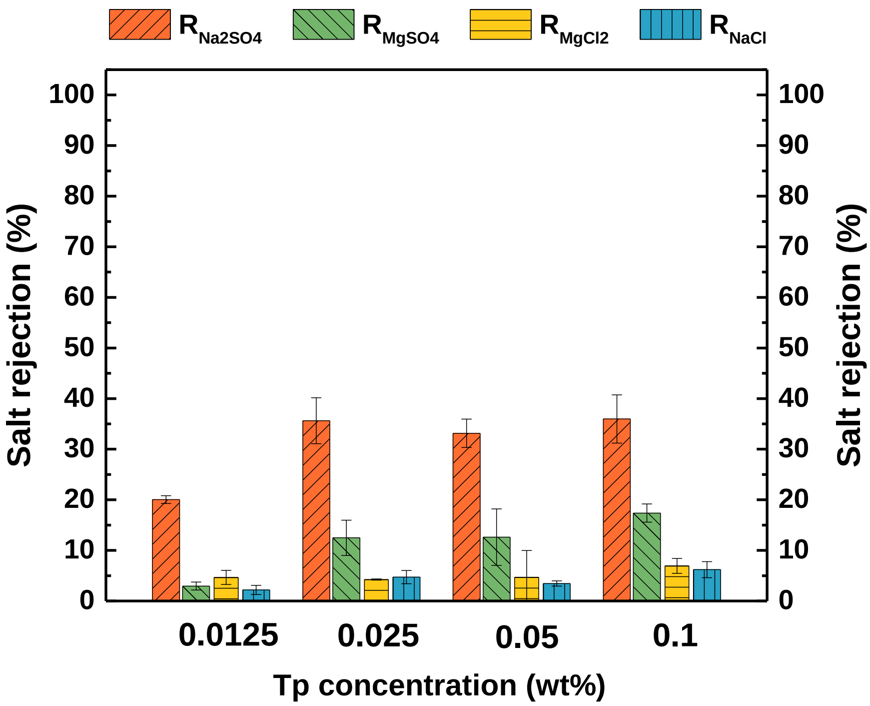

Figure 3. 14 Effect of Tp concentration on salt rejection performance.

3.4 Effect of Reaction Time on COF Morphology and Performance

The reaction time between Pa-2 and Tp monomers was changed (15, 30, 60, and 120 seconds) in this section. The Tp concentration was constant at 0.025wt%. Condition of Pa-2 concentration was 2wt% and Pa-2 soaking time was 30 seconds. As shown in Figure 3. 15, when increasing the reaction time from 15 seconds to 2 minutes, the COF membrane color changes slightly from camel to reddish-orange.

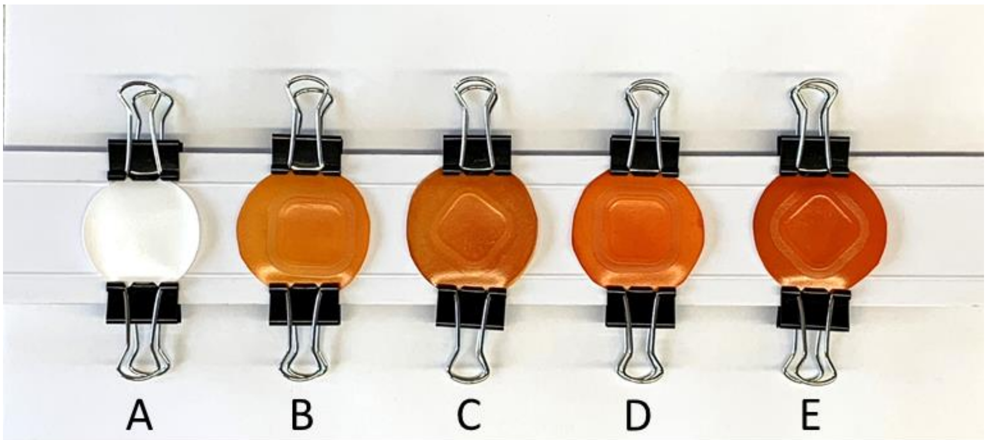

Figure 3. 15 Digital photo of various Tp reaction times of COF membrane. (A) Support (B) 15 sec, (C) 30 sec, (D) 60 sec, (E) 120 sec.

In the SEM images shown in Figure 3. 16. Pores can be found on all conditions of the membrane surface. However, the pore density decreases when increasing the reaction time. In addition, the pore size of the COF membrane decreases from 30 seconds to 60 seconds and is slightly smaller when the reaction time increase to 120 seconds. The reason for this result is that Tp monomers can have more time to form the COF layer on the support when increasing the reaction time during the interfacial polymerization step. During the polymerization step, the Tp monomers will be consumed at the interface between the aqueous and organic phase. Under a higher Tp reaction time, monomers can diffuse from the regions with a higher Tp concentration to replenish the Tp monomers at the interface, leading to more reactions occurring between the two phases.

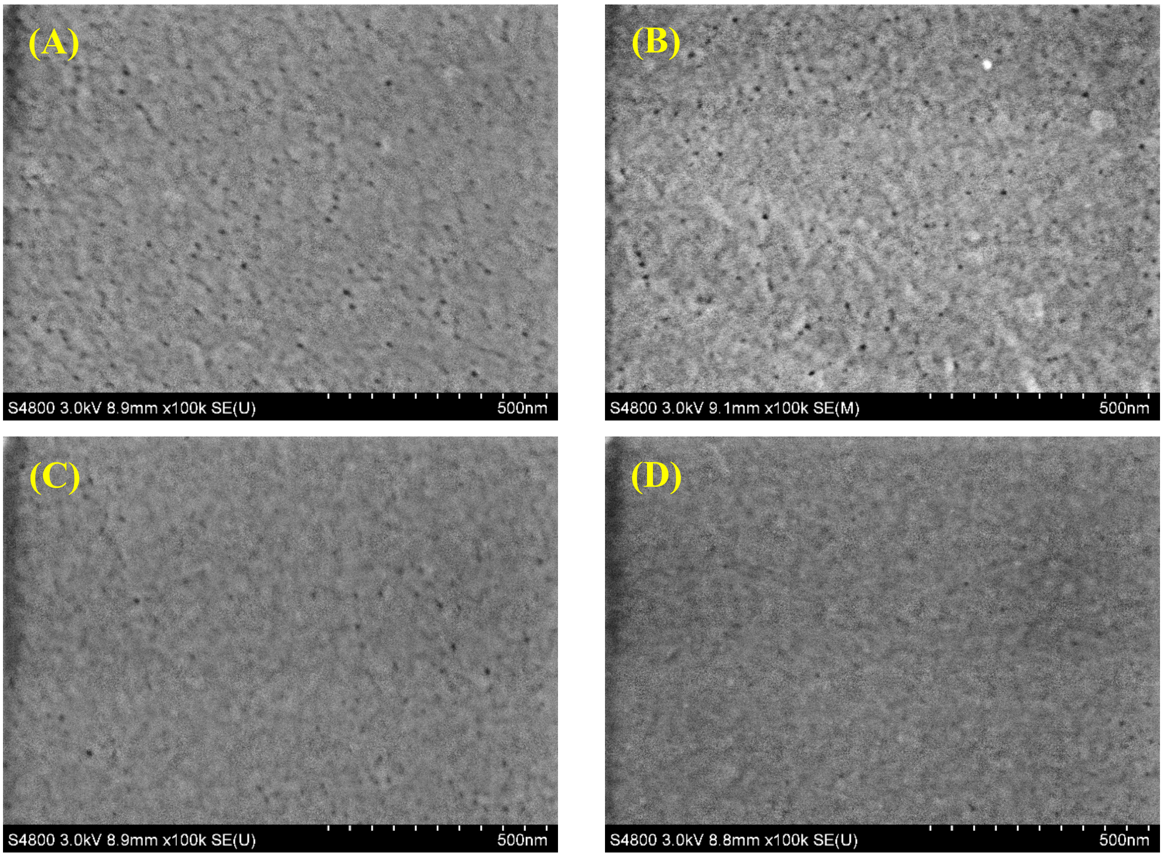

Figure 3. 16 Effect of Tp reaction time on SEM surface image. (A) 15 sec, (B) 30 sec, (C) 60 sec, (D) 120 sec.

The thickness of the COF layer is listed in Table 3. 4. With increasing the reaction time between Tp monomers and Pa-2 monomers from 15 seconds to 120 seconds, the thickness of the COF layer increases two times. In a longer reaction time of two monomers, the COF layer got more time to form on the support increasing the membrane thickness.

Table 3. 4 Effect of Tp reaction time on COF membrane thickness.

Tp reaction time (sec)	Thickness (nm)
15	361±72
30	567±93
60	666±87
120	846±90

The pure water flux of the COF membrane is shown in Figure 3. 17. The figure shows that the flux decreases with increasing the Tp reaction time. The pure water flux drops from 42 to 20 LMH/bar when the Tp reaction time increase from 15 to 120 seconds. In Figure 3. 16, the SEM images show a denser membrane surface, and in Table 3. 4, the membrane becomes thicker at a longer Tp reaction time. Due to higher resistance, the water will need more driving force to pass the membrane, leading to the flux being lower at a longer Tp reaction time.

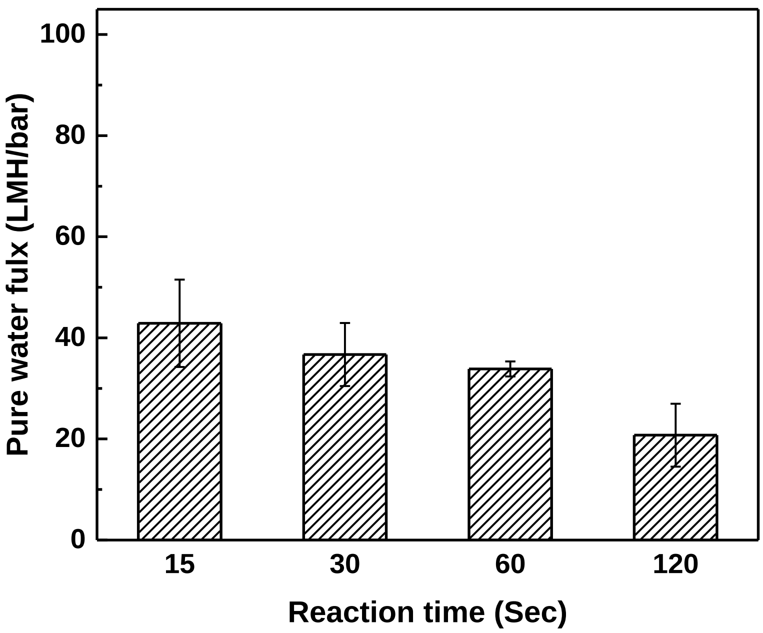

Figure 3. 17 Effect of Tp reaction time on pure water flux.

Figure 3. 18 shows the salt rejection performance of COF membranes. In this figure, we noticed the rejection of sodium sulfate increase with increasing the Tp reaction time. From the SEM in Figure 3. 16 and the thickness in Table 3. 4, the resistance of the membrane becomes higher with increasing the Tp reaction time. Improving the transfer resistance will also increase the selectivity of the COF membrane to the solute. The solutes are blocked upstream of the membrane, leading to a higher rejection of the salts.

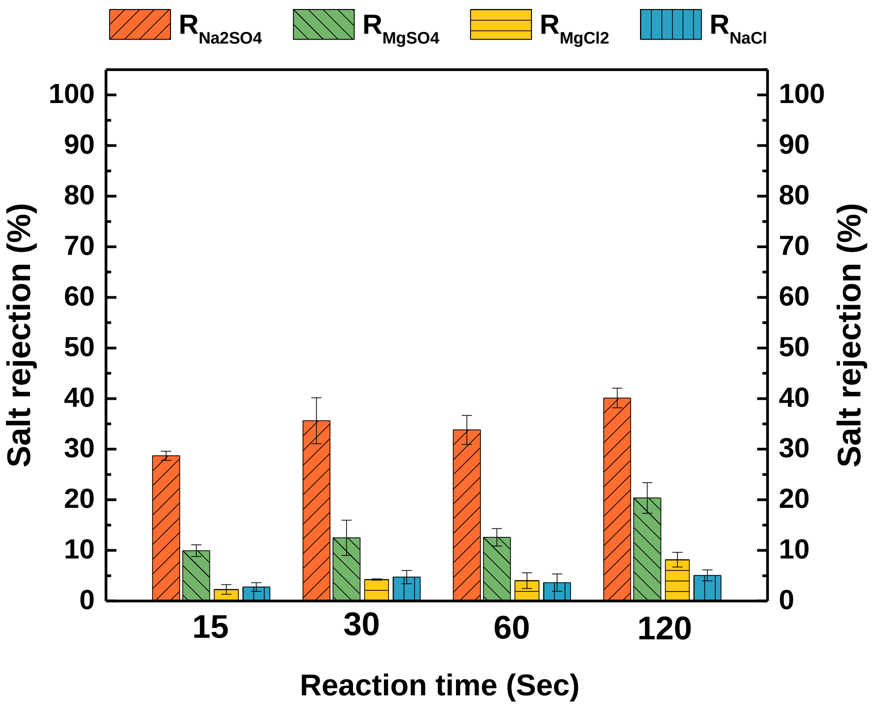

Figure 3. 18 Effect of Tp reaction time on salt rejection performance.

3.5 COF Membrane PFAS Removal Performance

The following figures show the PFAS removal performance of different COF membranes. Figure 3. 19 and 錯誤！找不到參照來源。 show the effects of Pa-2 concentration and Pa-2 soaking time on membrane performance. Three PFAS compounds were used to test the performance in this research, which were listed in Table 2. 1. The molecular weight of each PFAS can be found in this table, and the order is PFBS<PFOA<PFOS. Therefore, PFOS has the highest molecular weight, leading to a higher rejection shown in the following figures according to the sieving effect. PFBS has the lowest molecular weight among all PFAS tested and thus has the lowest rejection in all cases. It is interesting to see that all membranes exhibited similar PFBS rejection of around 65%, while the rejection of PFOS increased from 69.94% to 82.62% when the Pa-2 concentration increased from 0.25wt% to 2.0wt%. However, when the soaking time of the Pa-2 monomer increases, the PFOS rejection keeps constant at around 84%.

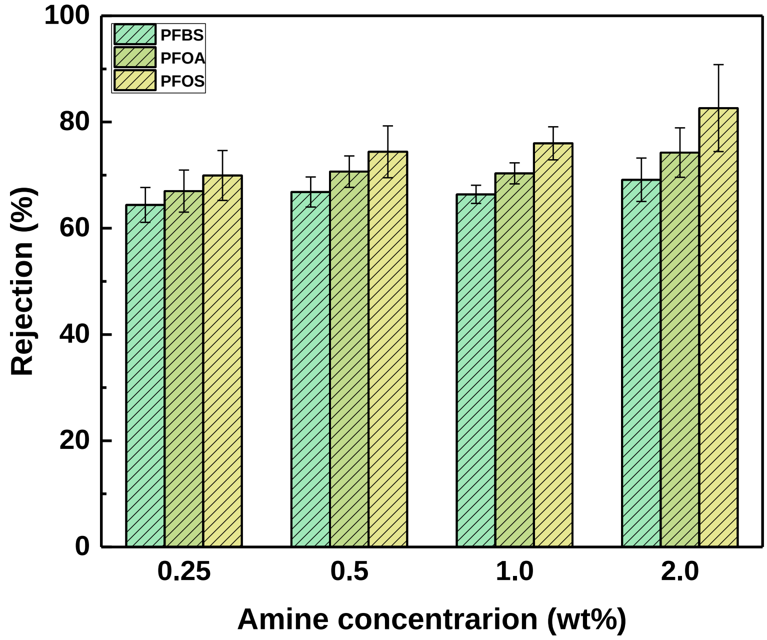

Figure 3. 19 Effect of Pa-2 concentration on PFAS removal performance.

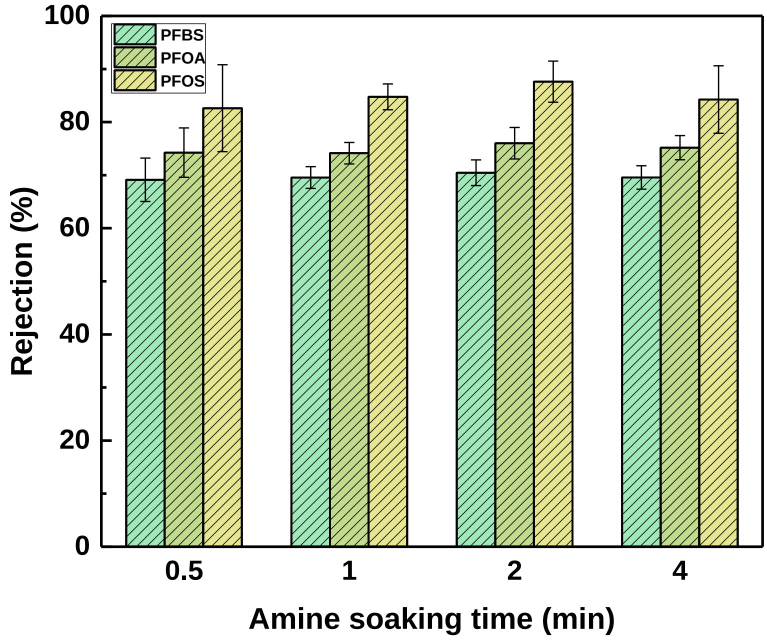

Figure 3. 20 Effect of Pa-2 soaking time on PFAS removal performance.

In Figure 3. 21, when increasing the Tp concentration, the rejection of all PFAS rejection rises quite significantly. When the concentration was 0.0125wt%, the rejection of PFASs was close to 64%. Nonetheless, as Tp concentration was increased, rejection of PFASs has varying degrees of increment according to the different molecular weights of PFAS.

In Figure 3. 22, when the reaction time was 15 seconds the PFOS rejection were only 60.18%. However, when the Tp reaction time increases to 120 seconds the highest PFOS rejection of 95.16% were obtained. There were similar results shown in Figure 3. 18. The salt rejection was higher when the Tp reaction time was 120 seconds. Other factors discussed in the previous section, including a thicker membrane and a denser membrane surface, will also contribute to the enhancement of PFAS rejection.

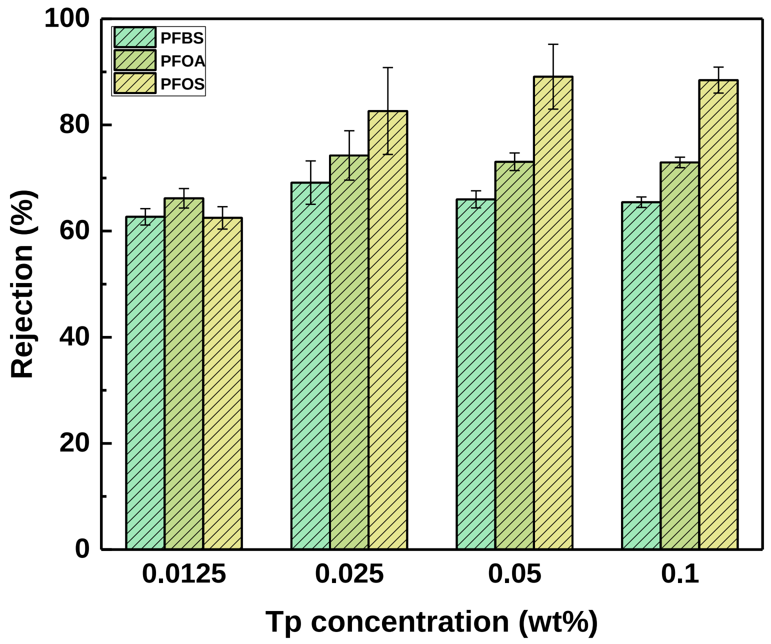

Figure 3. 21 Effect of Tp concentration on PFAS removal performance.

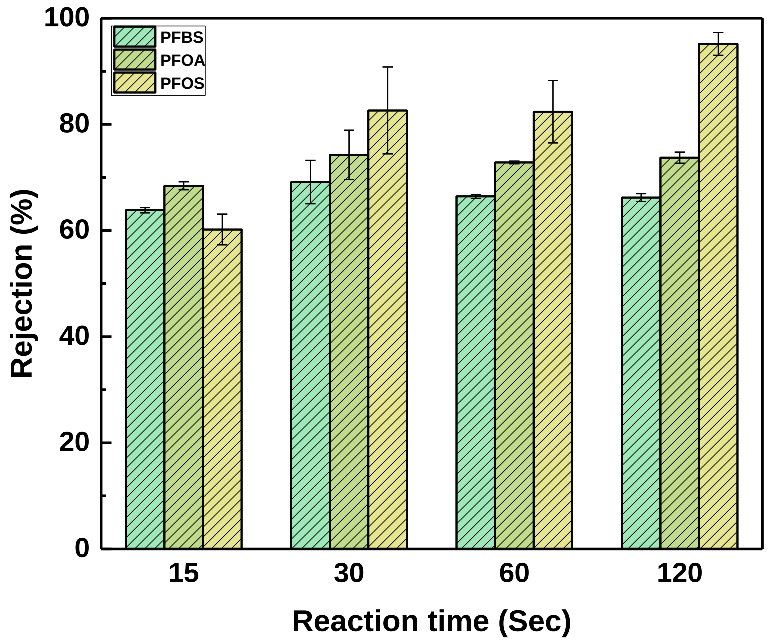

Figure 3. 22 Effect of reaction time on PFAS removal performance.

In the figure below, we have compiled the membrane thicknesses and PFOS rejctions of all membranes synthesized in this work. It can be seen that changing the Tp concentration and the reacton time have the greatest effect on membrane thickness. In addition, an interesting correlation can be observed between PFOS rejection and membrane thickness. There appears to be a critical thickness value around 1 μm, below which the PFOS rejection increases as the increase of membrane thickness. No further enhancement in the PFOS rejection was observed beyond 1 μm. This suggests that increasing thickness is effective in reducing non-selective defects inside the membrane and defect-free membrane can be obtained around the 1 μm. The thickness-rejection relationship may also indicate a correlation between the membrane thickness and the effective membrane pore size, which will be further investigated in our future work.

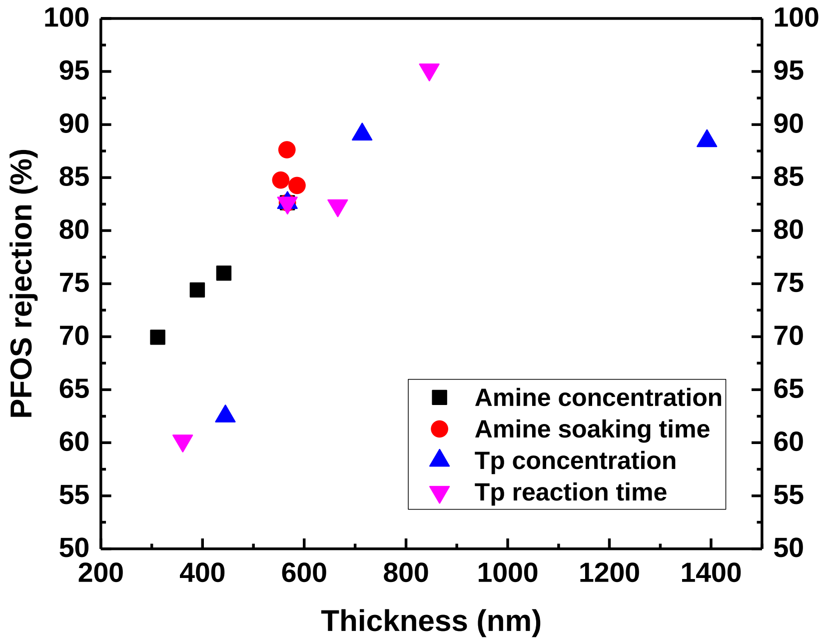

Figure 3. 23 PFOS rejection as a function of membrane thickness.

CHAPTER 4

CONCLUSIONS

In this research, the effect of various synthetic parameters on the morphology and separation performance of COF membranes were studied. The Pa-2 monomer was changed in the first two sections, including the monomer concentration and the soaking time. Here, we found that increasing the aqueous Pa-2 monomer concentration decreased the pure water flux slightly and increased the rejection of salts and PFAS. However, increasing the soaking time of the Pa-2 monomer did not have obvious effect on membrane surface morphology, membrane thickness, or membrane performances. The membrane morphology has significant differences when increasing the Tp concentration or the reaction time between Pa-2 and Tp monomers. SEM images showed that the COF membrane became denser and had less defects on the membrane surface as the Tp concentration or reaction time was increased. Similar results were observed for the membrane thickness. Changing the Tp monomer conditions led to different membrane thicknesses. The best performing COF membrane was obtained when increasing the reaction time to 120 seconds, and it showed the highest rejection of PFOS at 95.17%.

CHAPTER 5

FUTURE WORK

There are many factors that need to be considered when preparing covalent organic framework membrane by interfacial polymerization. Only a few of them were investigated in this work. Here we found that each condition has a different degree of influence on the membrane morphology and performance. The effect of other synthetic parameters will be studied in the future, including the type of solvent, the type and concentration of catalyst, and post-treatment. Regarding the separation mechanism, we hypothesized that both size exclusion and Donnan effects contribute to the promising PFAS rejection performance demonstrated by the COF membranes prepared in this work. Systematic membrane characterizations are being conducted to obtain the pore size distribution and membrane surface zeta potential information.

REFERENCES

[1] K. Kato, A.A. Kalathil, A.M. Patel, X. Ye, A.M. Calafat, Per- and polyfluoroalkyl substances and fluorinated alternatives in urine and serum by on-line solid phase extraction–liquid chromatography–tandem mass spectrometry, Chemosphere, 209 (2018) 338-345.

[2] A. Tkaczyk, K. Mitrowska, A. Posyniak, Synthetic organic dyes as contaminants of the aquatic environment and their implications for ecosystems: A review, Science of The Total Environment, 717 (2020) 137222.

[3] K.V. Kotsanopoulos, I.S. Arvanitoyannis, Membrane Processing Technology in the Food Industry: Food Processing, Wastewater Treatment, and Effects on Physical, Microbiological, Organoleptic, and Nutritional Properties of Foods, Critical Reviews in Food Science and Nutrition, 55 (2015) 1147-1175.

[4] D. Ghernaout, N. Elboughdiri, Water reuse: emerging contaminants elimination—Progress and trends, Open Access Library Journal, 6 (2019) e5981.

[5] S. Gunatilake, Methods of removing heavy metals from industrial wastewater, Journal of Multidisciplinary Engineering Science Studies, 1 (2015) 12-18.

[6] S.F. Mohsenpour, S. Hennige, N. Willoughby, A. Adeloye, T. Gutierrez, Integrating micro-algae into wastewater treatment: A review, Science of The Total Environment, 752 (2021) 142168.

[7] H. Udriot, A. Araque, U. Von Stockar, Azeotropic mixtures may be broken by membrane distillation, The Chemical Engineering Journal and the Biochemical Engineering Journal, 54 (1994) 87-93.

[8] M. Mulder, J. Mulder, Basic principles of membrane technology, Springer Science & Business Media, 1996.

[9] J. Lin, W. Ye, M.-C. Baltaru, Y.P. Tang, N.J. Bernstein, P. Gao, S. Balta, M. Vlad, A. Volodin, A. Sotto, P. Luis, A.L. Zydney, B. Van der Bruggen, Tight ultrafiltration membranes for enhanced separation of dyes and Na2SO4 during textile wastewater treatment, Journal of Membrane Science, 514 (2016) 217-228.

[10] P. Kohli, M. Wirtz, C.R. Martin, Nanotube membrane based biosensors, Electroanalysis: An International Journal Devoted to Fundamental and Practical Aspects of Electroanalysis, 16 (2004) 9-18.

[11] B. Van der Bruggen, Microfiltration, ultrafiltration, nanofiltration, reverse osmosis, and forward osmosis, in: Fundamental Modelling of Membrane Systems, Elsevier, 2018, pp. 25-70.

[12] S.M. Hosseinifard, M.A. Aroon, B. Dahrazma, Application of PVDF/HDTMA-modified clinoptilolite nanocomposite membranes in removal of reactive dye from aqueous solution, Separation and Purification Technology, 251 (2020) 117294.

[13] H.M. Tham, T.-S. Chung, One-step cross-linking and tannic acid modification of

polyacrylonitrile hollow fibers for organic solvent nanofiltration, Journal of Membrane Science, 610 (2020) 118294.

[14] L.W. Jye, A.F. Ismail, Nanofiltration membranes: Synthesis, characterization, and applications, CRC Press, 2016.

[15] N. Lan, K.Y. Wang, M. Weber, C. Maletzko, T.-S. Chung, Investigation of novel molecularly tunable thin-film nanocomposite nanofiltration hollow fiber membranes for boron removal, Journal of Membrane Science, 620 (2021) 118887.

[16] Y. Lei, B.W. Zhang, B.F. Bai, X. Chen, T.S. Zhao, A transient model for vanadium redox flow batteries with bipolar membranes, Journal of Power Sources, 496 (2021) 229829.

[17] J. Sun, C. Hu, B. Wu, H. Liu, J. Qu, Improving ion rejection of graphene oxide conductive membranes by applying electric field, Journal of Membrane Science, 604 (2020) 118077.

[18] A.P. Cote, A.I. Benin, N.W. Ockwig, M. O'Keeffe, A.J. Matzger, O.M. Yaghi, Porous, crystalline, covalent organic frameworks, science, 310 (2005) 1166-1170.

[19] M.S. Lohse, T. Bein, Covalent organic frameworks: structures, synthesis, and applications, Advanced Functional Materials, 28 (2018) 1705553.

[20] W. Zhang, L. Zhang, H. Zhao, B. Li, H. Ma, A two-dimensional cationic covalent organic framework membrane for selective molecular sieving, Journal of Materials Chemistry A, 6 (2018) 13331-13339.

[21] S. Yuan, X. Li, J. Zhu, G. Zhang, P. Van Puyvelde, B. Van der Bruggen, Covalent organic frameworks for membrane separation, Chemical Society Reviews, 48 (2019) 2665-2681.

[22] X. Guan, F. Chen, Q. Fang, S. Qiu, Design and applications of three dimensional covalent organic frameworks, Chemical Society Reviews, 49 (2020) 1357-1384.

[23] P. Wang, Y. Peng, C. Zhu, R. Yao, H. Song, L. Kun, W. Yang, Single-Phase Covalent Organic Framework Staggered Stacking Nanosheet Membrane for CO2-Selective Separation, Angewandte Chemie International Edition, 60 (2021) 19047-19052.

[24] E. Kissa, Fluorinated surfactants and repellents, CRC Press, 2001.

[25] R.C. Buck, J. Franklin, U. Berger, J.M. Conder, I.T. Cousins, P. De Voogt, A.A. Jensen, K. Kannan, S.A. Mabury, S.P. van Leeuwen, Perfluoroalkyl and polyfluoroalkyl substances in the environment: terminology, classification, and origins, Integrated environmental assessment and management, 7 (2011) 513-541.

[26] E. Gagliano, M. Sgroi, P.P. Falciglia, F.G.A. Vagliasindi, P. Roccaro, Removal of poly- and perfluoroalkyl substances (PFAS) from water by adsorption: Role of PFAS chain length, effect of organic matter and challenges in adsorbent regeneration, Water Research, 171 (2020) 115381.

[27] B.C. Crone, T.F. Speth, D.G. Wahman, S.J. Smith, G. Abulikemu, E.J. Kleiner, J.G. Pressman, Occurrence of per-and polyfluoroalkyl substances (PFAS) in source water and their treatment in drinking water, Critical reviews in environmental science and technology,

49 (2019) 2359-2396.

[28] T.D. Appleman, C.P. Higgins, O. Quiñones, B.J. Vanderford, C. Kolstad, J.C. Zeigler-Holady, E.R. Dickenson, Treatment of poly-and perfluoroalkyl substances in US full-scale water treatment systems, Water research, 51 (2014) 246-255.

[29] O.S. Arvaniti, A.S. Stasinakis, Review on the occurrence, fate and removal of perfluorinated compounds during wastewater treatment, Science of the Total Environment, 524 (2015) 81-92.

[30] M. Ateia, A. Maroli, N. Tharayil, T. Karanfil, The overlooked short-and ultrashort-chain poly-and perfluorinated substances: A review, Chemosphere, 220 (2019) 866-882.

[31] G. Munoz, P. Labadie, F. Botta, F. Lestremau, B. Lopez, E. Geneste, P. Pardon, M.-H. Dévier, H. Budzinski, Occurrence survey and spatial distribution of perfluoroalkyl and polyfluoroalkyl surfactants in groundwater, surface water, and sediments from tropical environments, Science of the Total Environment, 607 (2017) 243-252.

[32] N.M. Crawford, S.E. Fenton, M. Strynar, E.P. Hines, D.A. Pritchard, A.Z. Steiner, Effects of perfluorinated chemicals on thyroid function, markers of ovarian reserve, and natural fertility, Reproductive Toxicology, 69 (2017) 53-59.

[33] J.L. Domingo, M. Nadal, Per-and polyfluoroalkyl substances (PFASs) in food and human dietary intake: a review of the recent scientific literature, Journal of agricultural and food chemistry, 65 (2017) 533-543.

[34] J.C. DeWitt, Toxicological effects of perfluoroalkyl and polyfluoroalkyl substances, Springer, 2015.

[35] M.F. Rahman, S. Peldszus, W.B. Anderson, Behaviour and fate of perfluoroalkyl and polyfluoroalkyl substances (PFASs) in drinking water treatment: a review, Water research, 50 (2014) 318-340.

[36] I. Ross, J. McDonough, J. Miles, P. Storch, P. Thelakkat Kochunarayanan, E. Kalve, J. Hurst, S. S. Dasgupta, J. Burdick, A review of emerging technologies for remediation of PFASs, Remediation Journal, 28 (2018) 101-126.

[37] K.H. Kucharzyk, R. Darlington, M. Benotti, R. Deeb, E. Hawley, Novel treatment technologies for PFAS compounds: A critical review, Journal of Environmental Management, 204 (2017) 757-764.

[38] Q. Yu, R. Zhang, S. Deng, J. Huang, G. Yu, Sorption of perfluorooctane sulfonate and perfluorooctanoate on activated carbons and resin: Kinetic and isotherm study, Water Research, 43 (2009) 1150-1158.

[39] S. Deng, Y. Nie, Z. Du, Q. Huang, P. Meng, B. Wang, J. Huang, G. Yu, Enhanced adsorption of perfluorooctane sulfonate and perfluorooctanoate by bamboo-derived granular activated carbon, Journal of Hazardous Materials, 282 (2015) 150-157.

[40] H. Sun, F. Li, T. Zhang, X. Zhang, N. He, Q. Song, L. Zhao, L. Sun, T. Sun, Perfluorinated compounds in surface waters and WWTPs in Shenyang, China: mass flows

and source analysis, Water Research, 45 (2011) 4483-4490.

[41] Z. Du, S. Deng, Y. Bei, Q. Huang, B. Wang, J. Huang, G. Yu, Adsorption behavior and mechanism of perfluorinated compounds on various adsorbents—A review, Journal of Hazardous Materials, 274 (2014) 443-454.

[42] F. Hao, W. Guo, A. Wang, Y. Leng, H. Li, Intensification of sonochemical degradation of ammonium perfluorooctanoate by persulfate oxidant, Ultrasonics sonochemistry, 21 (2014) 554-558.

[43] E. Shahsavari, D. Rouch, L.S. Khudur, D. Thomas, A. Aburto-Medina, A.S. Ball, Challenges and Current Status of the Biological Treatment of PFAS-Contaminated Soils, Front Bioeng Biotechnol, 8 (2021) 602040-602040.

[44] B.N. Nzeribe, M. Crimi, S. Mededovic Thagard, T.M. Holsen, Physico-chemical processes for the treatment of per-and polyfluoroalkyl substances (PFAS): a review, Critical Reviews in Environmental Science and Technology, 49 (2019) 866-915.

[45] F. Li, J. Duan, S. Tian, H. Ji, Y. Zhu, Z. Wei, D. Zhao, Short-chain per- and polyfluoroalkyl substances in aquatic systems: Occurrence, impacts and treatment, Chemical Engineering Journal, 380 (2020) 122506.

[46] T. Lee, T.F. Speth, M.N. Nadagouda, High-pressure membrane filtration processes for separation of Per- and polyfluoroalkyl substances (PFAS), Chemical Engineering Journal, 431 (2022) 134023.

[47] C.Y. Tang, Q.S. Fu, C.S. Criddle, J.O. Leckie, Effect of Flux (Transmembrane Pressure) and Membrane Properties on Fouling and Rejection of Reverse Osmosis and Nanofiltration Membranes Treating Perfluorooctane Sulfonate Containing Wastewater, Environmental Science & Technology, 41 (2007) 2008-2014.

[48] T. Wang, C. Zhao, P. Li, Y. Li, J. Wang, Fabrication of novel poly(m-phenylene isophthalamide) hollow fiber nanofiltration membrane for effective removal of trace amount perfluorooctane sulfonate from water, Journal of Membrane Science, 477 (2015) 74-85.

[49] J. Wang, L. Wang, C. Xu, R. Zhi, R. Miao, T. Liang, X. Yue, Y. Lv, T. Liu, Perfluorooctane sulfonate and perfluorobutane sulfonate removal from water by nanofiltration membrane: The roles of solute concentration, ionic strength, and macromolecular organic foulants, Chemical Engineering Journal, 332 (2018) 787-797.

[50] T. Le, E. Jamshidi, M. Beidaghi, M.R. Esfahani, Functionalized-MXene Thin-Film Nanocomposite Hollow Fiber Membranes for Enhanced PFAS Removal from Water, ACS Applied Materials & Interfaces, (2022).

[51] L. Xu, J. Xu, B. Shan, X. Wang, C. Gao, TpPa-2-incorporated mixed matrix membranes for efficient water purification, Journal of Membrane Science, 526 (2017) 355-366.

[52] S. Chandra, S. Kandambeth, B.P. Biswal, B. Lukose, S.M. Kunjir, M. Chaudhary, R. Babarao, T. Heine, R. Banerjee, Chemically stable multilayered covalent organic nanosheets from covalent organic frameworks via mechanical delamination, Journal of the American

Chemical Society, 135 (2013) 17853-17861.

[53] C.-Y. Zhu, C. Liu, J. Yang, B.-B. Guo, H.-N. Li, Z.-K. Xu, Polyamide nanofilms with linearly-tunable thickness for high performance nanofiltration, Journal of Membrane Science, 627 (2021) 119142.